JOURNAL OF SOLID STATE CHEMISTRY **134,** 128–131 (1997)
ARTICLE NO. SC977556

Crystal Structure of New Layered Oxysulfides: $Sr_3Cu_2Fe_2O_5S_2$ and Sr_2CuMO_3S (M = Cr, Fe, In)

W. J. Zhu and P. H. Hor

Department of Physics and Texas Center for Superconductivity, University of Houston, Houston, Texas 77204-5932

Received April 14, 1997; in revised form July 7, 1997; accepted July 15, 1997

New layered oxysulfides with alternating Cu_2S_2 and perovskite oxide layers have been synthesized and characterized. The perovskite oxide layers for $Sr_3Cu_2Fe_2O_5S_2$ and Sr_2CuMO_3S (M = Cr, Fe, In) are $(FeO_2)(SrO)(FeO_2)$ and $(MO_2)(SrO)(SrO)(MO_2)$, respectively. All Fe, Cr, and In cations are in a square-pyramidal coordination geometry. Magnetic measurement shows an antiferromagnetic ordering at 60 K for Sr_2CuCrO_3S. © 1997 Academic Press

INTRODUCTION

Layered oxychalcogenides and oxypnictides are relatively less explored systems as compared with layered oxides, chalcogenides, and pnictides. The renewed interest in the square transition-metal oxygen/chalcogen sublattice has led to further investigation of these two classes of materials, where interactions between these two types of layers are expected to affect their electronic and magnetic properties. The first layered manganese oxypnictides were reported by Brechtel *et al.* (1), which contain the square-planar MnO_2 layer. This class of materials, as represented by $Sr_2Mn_3As_2O_2$, has been extensively studied by Kauzlarich's group (2–5). $Na_2Ti_2Pn_2O$ (Pn = As, Sb) (6) is another unusual compound with an anti-K_2NiF_4 type structure, where Ti is octahedrally coordinated by two oxygen and four Pn anions. As for layered oxysulfides, a large family of such materials are known (7) based on the general formula $(RO)_n(M_xX_y)$, where R = rare earth, M = a IB, IIA, IVA, IVA, or VA element, and X = S or Se. However, those with transition-metal oxide layers are rare. The first example is $Na_{1.9}Cu_2Se_2 \cdot Cu_2O$ (8), a metallic copper oxide selenide with alternating anti-CuO_2 type Cu_2O and Cu_2Se_2 layers. Recently, we synthesized and characterized several new members, $A_2Cu_2MO_2S_2$ (M = Mn, Co, Zn; A = Sr, Ba) (9, 10). These compounds are isostructural with $Sr_2Mn_3As_2O_2$ (1) with the square-planar MO_2 layer interleaved with the Cu_2S_2 layer where the transition-metal M is very weakly bonding to S at its apical site. $Sr_2Cu_2CoO_2S_2$ exhibits interesting magnetic properties with consecutive magnetic transitions and spin-glass behavior at low temperature. Resistive transitions were also observed in this material. Another interesting compound, Sr_2CuGaO_3S, was recently (11) prepared and determined to have a square-pyramidal GaO_5 layer. As a continuation of the investigation of this class of materials with other metal oxide layers, we report here the synthesis and structures of several new compounds: $Sr_3Cu_2Fe_2O_5S_2$ and Sr_2CuMO_3S (M = Cr, Fe, In).

EXPERIMENTAL

$Sr_3Cu_2Fe_2O_5S_2$ and Sr_2CuMO_3S (M = Cr, Fe, In) were synthesized from the stoichiometric amounts of materials listed in Table 1. Precursor SrS was prepared by hydrogen reduction of $SrSO_4$ at 900°C for 24 hr with intermittent grindings. $SrCuO_2$ and $Sr_2In_2O_5$ were obtained respectively by reacting $SrCO_3$ and CuO/In_2O_3. All samples were synthesized in evacuated quartz tubes. The colors of the resulting products are also listed in Table 1. X-ray diffraction characterization was performed on a Rigaku Dmax diffractometer. Intensity data were collected using Cu$K\alpha$ radiation in the angular range $2\theta = 15°$–$105°$ at steps of 0.02° and a counting time of 10 sec. The structure model is built on the concept of layer stacking of anti-PbO type Cu_2S_2 and perovskite oxide layers separated by Sr. Initial structure parameters were estimated by the bond valence rule (12). Structure refinement was performed using the DBW-9411 Rietveld program (13) with a pseudo-Voigt peak shape function. Preferred orientation along [001] was corrected using a March–Dollase function. Magnetic susceptibilities were measured between 5 and 300 K at 0.5 T on a SQUID (Quantum Design) magnetometer.

RESULTS AND DISCUSSION

(1) $Sr_3Cu_2Fe_2O_5S_2$

A single phase was obtained for $Sr_3Cu_2Fe_2O_5S_2$. All diffraction peaks can be indexed on a body-centered

0022-4596/97 $25.00

TABLE 1
Preparation Parameters for $Sr_3Cu_2Fe_2O_5S_2$ and Sr_2CuMO_3S (M = Cr, Fe, In)

Composition	Color	Starting materials	Conditions
$Sr_3Cu_2Fe_2O_5S_2$	Brown-red	SrS, $SrCuO_2$, Fe_2O_3, Cu	800°C, 12 hr
Sr_2CuCrO_3S	Yellow-green	SrS, $SrCuO_2$, Cr_2O_3, Cr	900°C, 12 hr
Sr_2CuFeO_3S	Red-brown	SrS, $SrCuO_2$, Fe_2O_3, Fe	850°C, 12 hr
Sr_2CuInO_3S	Brown	SrS, Cu_2O, $Sr_2In_2O_5$	900°C, 12 hr

tetragonal unit cell. Its lattice parameters were refined to be $a = 3.9115(10)$ Å and $c = 26.313(7)$ Å. Figure 1 shows its structure model, in which the Cu_2S_2 layer stacks alternately with the iron perovskite oxide layer $(FeO_2)(SrO)(FeO_2)$ separated by Sr. Rietveld refinement was performed on the structure and global parameters. Good agreement was achieved between the observed and calculated diffraction profiles (Fig. 2). Table 2 gives the atomic positional and displacement parameters and the derived atomic distances. As observed in $Sr_2Cu_2CoO_2S_2$, the relatively high displacement parameter for the Cu atom might be due to some Cu deficiency. The Fe–S bond distance (3.257 Å) is much longer than the sum of the ionic radii of Fe and S (2.48 Å), precluding a significant bonding between them. Fe can be viewed as being in square-pyramidal geometry. This kind of double square-pyramidal oxide sheet has also been observed in $YBaFeCuO_5$, $YBaCoCuO_5$, and $YBaMn_2O_5$, where the corresponding layers are $FeCuO_5$, $CoCuO_5$, and Mn_2O_5, respectively. All other bonding distances are within their normal values. The oxidation state of Fe in this compound is +3. Pure samples cannot be obtained at synthetic temperatures above 900°C because of the oxidation of S^{2-} by Fe^{3+} into sulfate SO_4^{2-}.

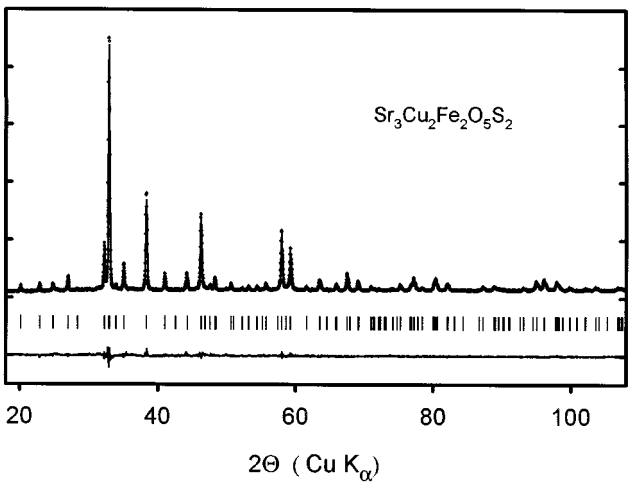

FIG. 2. Observed and calculated X-ray diffraction patterns for $Sr_3Cu_2Fe_2O_5S_2$ with differenceprofile shown below. The vertical bars indicate the reflection positions.

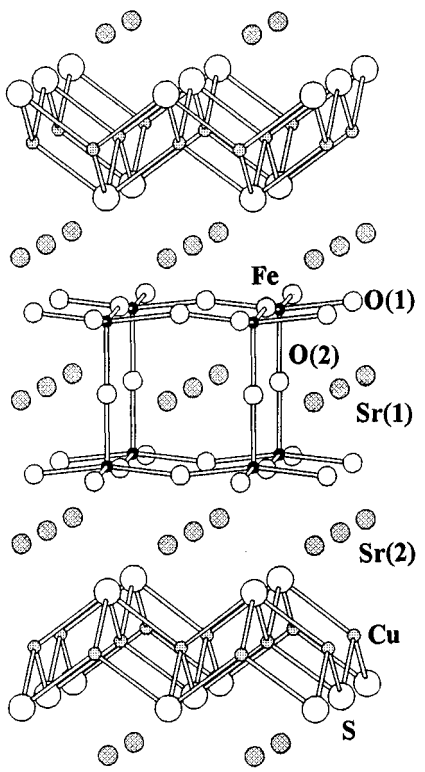

FIG. 1. Structure of $Sr_3Cu_2Fe_2O_5S_2$ with the Cu_2S_2 layer alternating withthe double square-pyramidal oxide layer Fe_2O_5.

TABLE 2
Atomic Positional and Isotropic Displacement Parameters (10^{-3} Å^2) for $Sr_3Cu_2Fe_2O_5S_2$ and Derived Atomic Distances (Å) (Space Group: *I4/mmm*)

Atom	x	y	z	U
Fe	0	0	0.0718(1)	2.5(9)
Cu	$\frac{1}{2}$	0	$\frac{1}{4}$	10.1(9)
Sr(1)	$\frac{1}{2}$	$\frac{1}{2}$	0	5.6(8)
Sr(2)	$\frac{1}{2}$	$\frac{1}{2}$	0.1418(1)	3.3(6)
S	0	0	0.1956(1)	1.3(1)
O(1)	$\frac{1}{2}$	0	0.0798(3)	6.3(3)
O(2)	0	0	0	1.3(1)

Fe–O(1) (×4)	1.967(1)	Sr(1)–O(1) (×8)	2.869(6)
Fe–O(2) (×1)	1.889(2)	Sr(1)–O(2) (×4)	2.766(1)
Fe–S (×1)	3.257(3)	Sr(2)–S (×4)	3.107(2)
Cu–S (×4)	2.423(1)	Sr(2)–O(1) (×4)	2.547(5)

Note. $R_p = 3.65\%$, $R_{wp} = 4.87\%$, $R_E = 5.24\%$, $S = 0.93$, $R_B = 4.65\%$, $R_F = 3.76\%$.

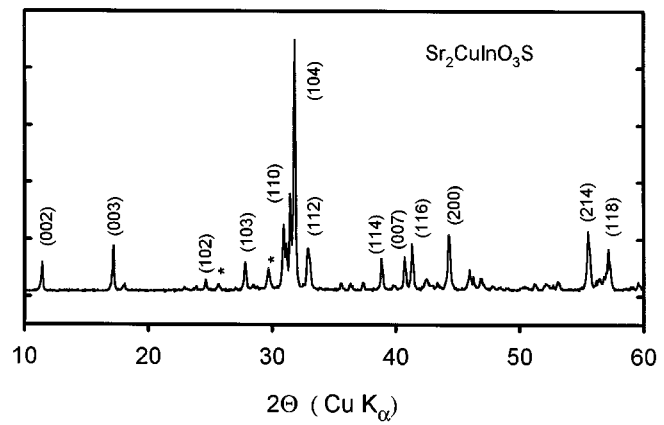

FIG. 3. X-ray diffraction pattern for Sr_2CuInO_3S with minor impurity peaksdue to SrS and strontium indium oxides.

(2) *Sr_2CuMO_3S (M = Cr, Fe, In)*

A Single phase was obtained for $Sr_2Cu\mathit{M}O_3S$ (M = Cr, Fe) except for M = In. These are some minor impurity peaks (Fig. 3) due to SrS and strontium indium oxides. This series is isostructural with Sr_2CuGaO_3S (11) with two square-pyramidal oxide layers alternating with Cu_2S_2 (Fig. 4). Their lattice parameters are listed in Table 3. Structure refinement for $Sr_2Cu\mathit{M}O_3S$ (M = Cr, Fe) gives a good fit between the observed and calculated diffraction profiles (Fig. 5). Table 4 lists the atomic positional and displacement parameters, with the calculated atomic distances in Table 5. Again, the Cu atom shows a large displacement, indicating that Cu deficiency is a common feature in this class of materials. Long distances between trivalent Fe^{3+}, Cr^{3+}, and their apical S^{2-} suggested no significant bonding between these atoms. For Fe and Cr, the square-pyramidal coordination geometry can be found in their othe compounds. Although we have not yet obtained a pure

TABLE 3
Lattice Parameters (Å) for $Sr_2Cu\mathit{M}O_3S$ (M = Cr, Fe, In)

	M		
Paremeter	Cr	Fe	In
a	3.9000(6)	3.8951(11)	4.091(1)
c	15.333(3)	15.613(5)	15.473(5)

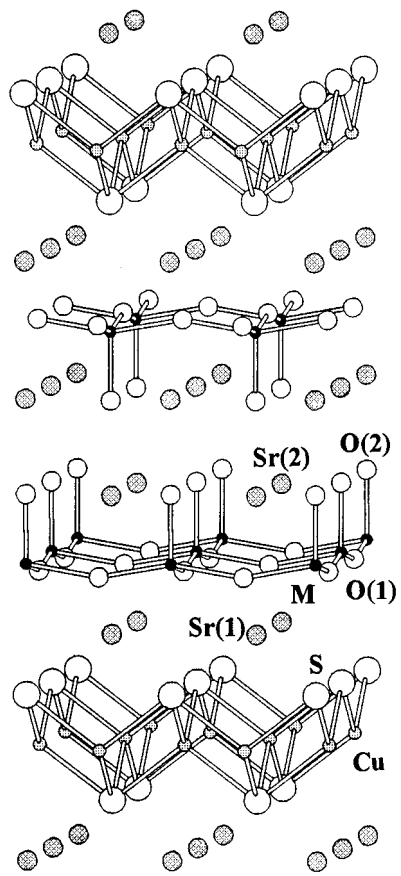

FIG. 4. Structure of $Sr_2Cu\mathit{M}O_3S$ (M = Cr, Fe, In), showing alternate stacking of the Cu_2S_2 and square-pyramidal MO_3 layers.

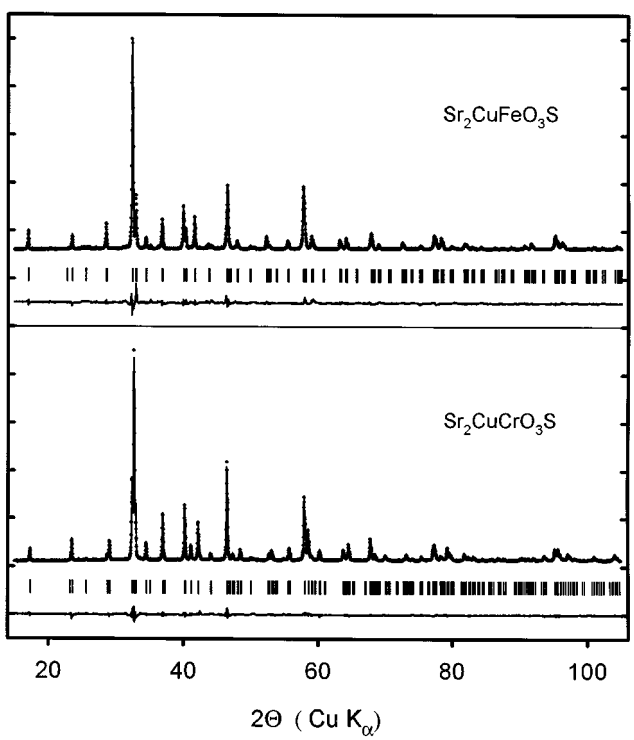

FIG. 5. Observed and calculated X-ray diffraction patterns for $Sr_2Cu\mathit{M}O_3S$ (M = Cr, Fe) withdifference profiles shown below. The vertical bars indicate the reflection positions.

TABLE 4
Atomic Coordinates and Isotropic Displacement Parameters (10^{-3} Å^2) for Sr_2CuMO_3S (M = Cr, Fe) (Space Group: *P4/nmm*)

			M = Cr		M = Fe	
Atom	x	y	z	U	z	U
M	$\frac{1}{4}$	$\frac{1}{4}$	0.3053(3)	4.2(9)	0.3128(4)	3.5(7)
Cu	$\frac{1}{4}$	$\frac{1}{4}$	0	8.9(3)	0	10.2(3)
Sr(1)	$-\frac{1}{4}$	$-\frac{1}{4}$	$0.18\frac{1}{4}54(1)$	3.3(6)	0.1871(3)	4.8(9)
Sr(2)	$-\frac{1}{4}$	$-\frac{1}{4}$	0.4126(1)	3.8(6)	0.4138(2)	4.7(9)
S	$\frac{1}{4}$	$\frac{1}{4}$	0.0966(3)	2.5(1)	0.0959(7)	8.8(3)
O(1)	$\frac{1}{4}$	$-\frac{1}{4}$	0.2889(5)	7.6(3)	0.2887(7)	8.9(3)
O(2)	$\frac{1}{4}$	$\frac{1}{4}$	0.4256(6)	10.1(4)	0.4350(10)	9.8(4)

Note. $R_{wp} = 5.08\%$, $S = 0.95$, and $R_F = 3.92\%$ for M = Cr and $R_{wp} = 7.85\%$, $S = 1.19$, and $R_F = 6.34\%$ for M = Fe.

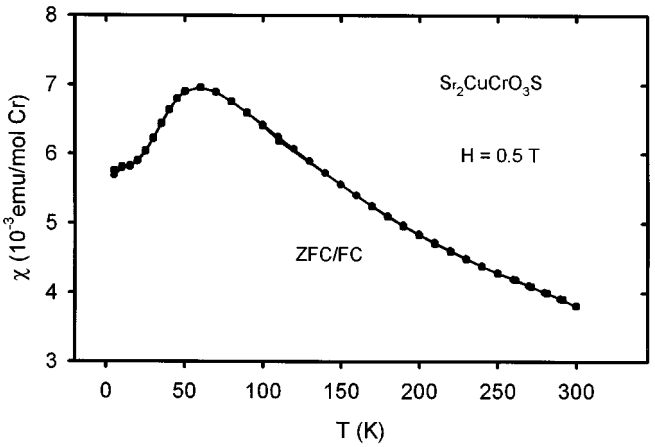

FIG. 6. Magnetic susceptibility for Sr_2CuCrO_3S measured at 0.5 T.

In-containing phase for structure parameter determination, we expect that In will also assume this kind of coordination geometry. The successful realization of this kind structure is attributed to the good geometrical and charge compatibility of the rigid layer $(Cu_2S_2)^{2-}$ and the perovskite oxide layer $[(MO_3)(SrO)(SrO)(MO_3)]^{2-}$ with Sr^{2+} in between. Sr is well above the S plane that is perpendicular to the c axis, driving the next MO_3 layer far apart from the S plane. Although X-ray diffraction analysis cannot determine possible partial antidoping between the Cu^+ and trivalent M^{3+} sites, the unreasonably high atomic valence for monovalent Cu^+ at the M^{3+} site precludes this possibility. It was estimated to be 1.86, 1.92, and 1.78 for $Sr_3Cu_2Fe_2O_5S_2$, Sr_2CuCrO_3S, and Sr_2CuFeO_3S, respectively. Direct evidence will rely on further neutron diffraction experiments.

Resistivity measurement shows that all these $Sr_3Cu_2Fe_2O_5S_2$ and Sr_2CuMO_3S (M = Cr, Fe, In) phases are insulating. Magnetic susceptibility of Sr_2CuCrO_3S (Fig. 6) exhibits a broad maximum at about 60 K, indicating a low-dimensional antiferromagnetic ordering of Cr^{3+} of the CrO_3 square-pyramidal layer. Fitting the data above 150 K to the Curie–Weiss law gives a paramagnetic temperature of $-175(4)$ K and an effective moment of 3.81 μ_B, which corresponds to the spin $S = \frac{3}{2}$ of Cr^{3+} $3d^3$.

In summary, new layered oxysulfides $Sr_3Cu_2Fe_2O_5S_2$ and Sr_2CuMO_3S (M = Cr, Fe, In) have been synthesized and their structures determined. All of them contain a square-pyramidal oxide layer. This kind of configuration is unusual for In in an extended structure. Further investigation on new members of this class of materials and doping studies to explore novel electronic and magnetic properties are in progress.

TABLE 5
Atomic Distances (Å) for Sr_2CuMO_3S (M = Cr, Fe)

Atom–atom	M = Cr	M = Fe
M–O(1) ($\times 4$)	1.966(1)	1.984(2)
M–O(2) ($\times 1$)	1.845(10)	1.907(15)
M–S ($\times 1$)	3.200(6)	3.386(12)
Cu–S ($\times 4$)	2.448(3)	2.456(6)
Sr(1)–O(1) ($\times 4$)	2.514(5)	2.512(7)
Sr(1)–S ($\times 4$)	3.075(2)	3.100(5)
Sr(2)–O(1) ($\times 4$)	2.720(5)	2.758(8)
Sr(2)–O(2) ($\times 1$)	2.481(9)	2.361(16)
Sr(2)–O(2) ($\times 4$)	2.765(1)	2.774(2)

ACKNOWLEDGMENTS

This work was supported by NSF Low Temperature Physics Program Grant DMR 9122043, ARPA Grant MDA 972-90-J-1001, and the Texas Center for Superconductivity at the University of Houston.

REFERENCES

1. E. Brechtel, G. Cordier, and H. Schäfer, *Z. Naturforsch. B* **34,** 777 (1979).
2. N. T. Stetson and S. M. Kauzlarich, *Inorg. Chem.* **30,** 3969 (1991).
3. S. L. Brock and S. M. Kauzlarich, *Inorg. Chem.* **33,** 2491 (1994).
4. S. L. Brock, N. P. Raju, J. E. Greedan, and S. M. Kauzlarich, *J. Alloys Compd.* **237,** 9 (1996).
5. S. L. Brock and S. M. Kauzlarich, *J. Alloys Compd.* **241,** 82 (1996).
6. A. Adam and H.-U. Schuster, *Z. Allorg. Allg. Chem.* **584,** 150 (1990).
7. M. Guittard, S. Benazeth, J. Dugué, S. Jaulmes, M. Palazzi, P. Laruelle, and J. Flahaut, *J. Solid State Chem.* **51,** 227 (1984).
8. Y. Park, D. C. Degroot, J. L. Schindler, C. R. Kannewurf, and M. G. Kanatzidis, *Chem. Mater.* **5,** 8 (1993).
9. W. J. Zhu, P. H. Hor, A. J. Jacobson, G. Crisci, T. A. Albright, S.-H. Wang, and T. Vogt, *J. Am. Chem. Soc.*, in press.
10. W. J. Zhu and P. H. Hor, *J. Solid State Chem.* **130,** 319 (1997).
11. W. J. Zhu and P. H. Hor, *Inorg. Chem.* **36,** 3576 (1997).
12. I. D. Brown and D. Altermatt, *Acta Crystallogr. B* **41,** 244 (1985).
13. R. A. Young, A. Sakthivel, T. S. Moss, and C. O. Paiva-Santos, *J. Appl. Crystallogr.* **28,** 366 (1995).